

This article was downloaded by:

On: 25 January 2011

Access details: *Access Details: Free Access*

Publisher *Taylor & Francis*

Informa Ltd Registered in England and Wales Registered Number: 1072954 Registered office: Mortimer House, 37-41 Mortimer Street, London W1T 3JH, UK



Liquid Crystals

Publication details, including instructions for authors and subscription information:

<http://www.informaworld.com/smpp/title~content=t713926090>

The optical response of liquid crystal cells to a low frequency driving voltage

Stephen Palmer

Online publication date: 06 August 2010

To cite this Article Palmer, Stephen(1998) 'The optical response of liquid crystal cells to a low frequency driving voltage', *Liquid Crystals*, 24: 4, 587 – 598

To link to this Article: DOI: 10.1080/026782998207064

URL: <http://dx.doi.org/10.1080/026782998207064>

PLEASE SCROLL DOWN FOR ARTICLE

Full terms and conditions of use: <http://www.informaworld.com/terms-and-conditions-of-access.pdf>

This article may be used for research, teaching and private study purposes. Any substantial or systematic reproduction, re-distribution, re-selling, loan or sub-licensing, systematic supply or distribution in any form to anyone is expressly forbidden.

The publisher does not give any warranty express or implied or make any representation that the contents will be complete or accurate or up to date. The accuracy of any instructions, formulae and drug doses should be independently verified with primary sources. The publisher shall not be liable for any loss, actions, claims, proceedings, demand or costs or damages whatsoever or howsoever caused arising directly or indirectly in connection with or arising out of the use of this material.

The optical response of liquid crystal cells to a low frequency driving voltage

by STEPHEN PALMER

Hörnell Innovation AB, Tunavägen 281, 781 73 Borlänge, Sweden

(Received 21 July 1997; accepted 29 October 1997)

This study investigates the optical response of liquid crystal cells to a low frequency square wave voltage of 0.1 Hz. It is found that there are three physical phenomena that dominate the overall properties of the device. The first is the discharging effect whereby the effective voltage over the liquid crystal layer decreases as a function of time; this occurs due to mobile ions being present within the liquid crystal material. The second is the charging-up of the cell where the effective voltage increases with time; this is attributed to charge separation taking place within the polyimide layer upon application of the d.c. voltage component. The third effect is cell asymmetry whereby the effective voltage depends upon the polarity of the externally applied field; this is the result of a locked-in d.c. holding voltage being present within the cell layers. These three effects are analysed in some detail with the view of developing a liquid crystal cell capable of being driven with a low frequency square wave voltage. A model of a liquid crystal cell in which the liquid crystal material can dissolve impurity ions from the alignment layers and in which the ions can then become re-adsorbed into the polyimide layer is deduced.

1. Introduction

Liquid crystal displays (LCDs) are conventionally driven with square wave voltages of 40 Hz or more. This prevents impurity ion migration from occurring within the cell, an effect that can otherwise cause the long term degradation of the electro-optic properties. The actual response of the device is dependent upon the rms of the effective field acting over the liquid crystal material and not on the polarity. However, the charge–discharge cycling of the cell commands a large power consumption, particularly undesirable for battery operated devices. Reduction of the driving frequency has beneficial effects upon the current drain of the display but also places a high demand on the quality of the cell in order to reduce the chemical degradation processes to a minimum.

The ionic transport mechanisms occurring within an LCD are also important. The simplified model of a liquid crystal cell being represented by a parallel RC circuit assumes that the ionic concentration of the liquid crystal material and the mobility of the ions are constant. A refinement of this model uses three such RC circuits connected in series, one for each of the two polyimide layers and one for the slab of liquid crystal material. A serial resistor is also required in order to simulate the ITO contacting layers.

However, it is found that such a model is only appropriate when the resistivity of the liquid crystal material is sufficiently small that the product of the

driving voltage, V and the resistivity, ρ_{LC} satisfied the equation $V\rho_{LC} < 10^9 \text{ V } \Omega \text{ m}$ [1, 2]. In this region, the ionic concentration is sufficiently high for the resistivity of the liquid crystal material to be considered as being time independent. With such a model, it is found that when using low driving frequencies the effective voltage across the liquid crystal material decreases both with a decreasing liquid crystal resistivity and an increasing polyimide thickness. Now, modern halogenated liquid crystal materials can be purified to the extent that their residual resistivities reach values of high quality insulators and often it is found that the above inequality is not satisfied. Here, the limited number of impurity ions results in a liquid crystal resistivity that is time dependent, producing a large deviation from the results predicted by the RC-circuit model above.

Transient current measurement techniques [3] can be used to investigate the leakage currents flowing in LCDs. Experiments demonstrate that it is possible to detect the existence of at least two oppositely charged, mobile ions moving within the liquid crystal material [4, 5] and confirm that charge transport mechanisms strongly affect the optical properties of LCDs. In particular, an increasing ionic content causes the threshold voltage to rise [6]. Impurity ions have different mobilities due to their geometric size. In order to obtain a theoretical fit to the experimental data, it is also necessary to introduce the idea of ion trapping at the alignment layer

boundaries [7, 8]. Here, the ions are considered to be absorbed at the polyimide surface with a trapping speed K_{trap} and desorbed with a time constant τ .

Ionic contaminants can originate from the dissociations of impurities and neutral liquid crystal molecules under the excitation of an electric field. The measurement of the leakage current as a function of temperature enables the activation energies of these dissociation reactions to be determined. There is also evidence to indicate that ions can be dissolved by the liquid crystal material from the alignment layers [9] and it is found that the UV exposure of a polyimide film generates a decrease in the resistivity of a liquid crystal cell. The ionic solubility is dependent upon the $\Delta\epsilon$ parameter of the liquid crystal material. Contamination from the glass substrates can also occur where ionic exchange releases halide ions into the liquid crystal material and work has been carried out using barrier layers of SiO_2 to reduce this effect [10].

By combining a transient conduction model allowing for ionic trapping at the alignment layers together with the dynamic model for a liquid crystal cell, it is possible to analyse the optical behaviour of a nematic LCD [11]. The additional generation and recombination processes of dissociating molecules can also be included [12]. The application of an electric field causes the ions to separate and a net generation of ions appears because the recombination rate decreases at places in the liquid crystal layer where only one of the two ionic species remains. Transient current measurements indicate that the alignment layers can also be treated as perfect insulators and that the supplementary charge that is generated within the liquid crystal material cannot leak away through these layers.

There is a direct relationship between the resistivity of a liquid crystal material and the d.c. holding voltage, which causes the so-called *sticking effect* in a thin film transistor liquid crystal display [13]. This occurs when there are different quantities of ions trapped at the two polyimide surfaces and it is enhanced by there being an asymmetry in the trapping ratios of ions within the alignment layers [14]. It is also found that the thicker the alignment layer, the larger is the d.c. holding voltage. It is therefore important to minimize the ionic contamination of liquid crystal materials and it is found that the use of highly resistive, fluorinated liquid crystal materials together with highly imidified polyimide films dramatically reduces the d.c. holding voltage [15].

The liquid crystal resistivity is reflected by the voltage holding ratio (VHR) of the display. This parameter is defined as being the fraction of voltage remaining over a cell after a certain length of discharge time and can only change when either the resistivity of the liquid crystal material, R_{LC} or the capacitance of this layer, C_{LC} changes. The value of R_{LC} is dominated both by the

dielectric constants of the liquid crystal material and the ionic contamination of the polyimide layer. From the VHR values, it is seen that R_{LC} decreases by a factor of five when the initially applied voltage is increased from 1 to 10 V [16]. An additional effect of free ion injection from the polyimide layer is required to explain this result. The polyimide material influences the voltage dependency of the liquid crystal resistivity, demonstrating the importance of using an orienting layer with a minimal ionic pollution effect.

The optical transmission of an LCD can be used as a direct measurement of the effective rms voltage acting on the liquid crystal layer, enabling the time constants of the adsorption and desorption processes of impurity ions at the polyimide surfaces to be studied [17]. In a simple model, the rate of ion absorption can be taken as being proportional to $V_{\text{applied}} - V_{\text{ion}}$, where V_{applied} is the externally applied voltage and V_{ion} is the internal field set up by the trapped ions at the alignment layer boundaries. The rate of desorption is taken as being proportional to V_{ion} . It is often found that the release constants for the trapped ions are larger than those for the adsorption processes.

This report analyses the effective voltage acting on the liquid crystal layer when using low driving frequencies by monitoring the optical transmission of the display. The cells are driven with a 0.1 Hz square wave voltage ranging from ± 1 to ± 10 V in steps of ± 1 V and the transmittance of the device is measured as a function of time. For each voltage step, the transmittance is measured over a 20 s period encapsulating four polarity reversals of the driving voltage. The cells are placed between crossed Sanritz LC81 polarizers and an interference filter is present that possesses a high transmittance over the central part of the visible spectrum and eliminates both UV and IR radiation.

The transmittance of the cell is measured in units of shade numbers, S [18] which is related to the integrated luminous transmission, T expressed as a percentage by $S = (7/3) \log_{10}(100/T) + 1$. A luminous transmittance of 100% gives a shade number of 1.00 and as the transmission goes down, the shade number increases. This logarithmic scale ensures that perceived equal brightness steps are represented by equal steps in shade numbers.

From the optical response of the cells to low frequency driving, two parameters are obtained. The first represents the asymmetry of the device and is defined as the difference between the shade numbers attained by the cell immediately upon reversal of the voltage for the two different polarities. The second is referred to as the R value and represents the way in which the shade number of the cell changes under the action of a d.c. voltage. By definition, the R value is taken as being the difference between the shade numbers attained by the cell at the

beginning and end of each 5 s period of d.c. driving between polarity reversals of the applied voltage. A positive R value indicates that the shade number decreases with time (cell decay).

2. Measurement of the optical properties

In principle, the shade number S , of a filter is measured by monitoring the current output, I , from a photodetector and normalizing this value with the reference current, I_{ref} corresponding to 100% transmittance. If, for example, the unit is required to measure up to a shade number 14, from the definition of shade number we have $\log_{10}(I_{\text{ref}}/I) = (S - 1)(3/7)$ which yields $\log_{10}(I_{\text{ref}}/I) = 5.57$ for $S = 14$. A logarithmic amplifier is therefore required that is capable of dealing with input currents encapsulating at least 5.57 decades of magnitude ranging from 1 nA to 1 mA.

The equipment used to measure the luminous transmittance of samples consists of three parts: a photopic light detector, light source and a logarithmic amplifier. The standard light detector used is a Lichtmesstechnik LMT P10 FC photodetector. The head consists of a 10-mm-diameter silicon-based photoelement with a surface absorption spectrum adapted to match that of the sensitivity curve for the human eye during daytime viewing. The output current from the device is linearly proportional to the impinging radiation intensity. Its temperature sensitivity was insignificant for our purposes.

The photodetector is connected directly to a screened logarithmic amplifier module (Analogue Devices 755N) giving output voltages lying in the -5 to $+5$ V region and rises 1 V for every decade increase in input current. The exiting signal is passed through a precision rectifier and sampling of the resultant is carried out via utilization of a microprocessor card based on an Intel 80535 chip. The sampling size is made at 10 bits giving a resolution of 5 mV.

The radiation source employed is a 150 V halogen projector lamp running at 24 V and focused by a series of lenses to form an intense parallel beam of diameter 5 mm. This is concentrated onto the surface of the photodetector and the amplifier adjusted so as to give a reading of 1.00 corresponding to 100% transmittance. Positioning of the sample between the projector lamp and the detector enables the shade number of samples to be directly determined.

In order to ascertain the accuracy of the apparatus, several neutral density filters of known shade numbers were obtained from the Deutsches Institut für Normung† and measured using the experimental equipment. Direct comparison between the two sets of numbers enables the precision of the unit to be established. The results indicate that the errors lie below 0.50% over a wide range of transmittances up to and including shade number 14.

3. Results

It is found that the low frequency response of a liquid crystal cell is dominated by three basic phenomena: the discharge of the cell, charging-up of the cell and an asymmetry due to the presence of a locked-in d.c. holding voltage. A positive R value (cell decay) occurs due to mobile impurity ions present within the liquid crystal material. Applying a d.c. voltage enables the ions to migrate to the cell sides under the action of the electric field. The layer of ensuing charge screens the bulk liquid crystal material and lowers the effective voltage acting across the liquid crystal layer. When the cell is operating in the normally transparent mode, this results in a reduction of shade number as a function of time. The characteristics of a cell displaying this phenomenon

†Deutsches Institut für Normung Standards, Westliche 56, 7530 Pforzheim, Germany.

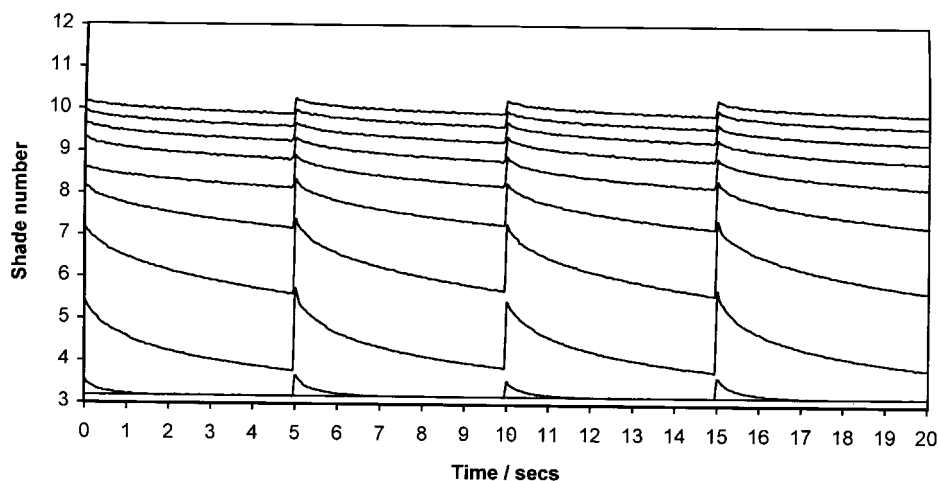


Figure 1. $4\ \mu\text{m}$ 80° LT cell with Merck ZLI-3700-000 liquid crystal component displaying the discharge effect (positive R value) due to mobile ions present within the liquid crystal material. The cell is placed between crossed LC81 polarizers and an interference filter is present. The cell is driven with a $\pm V$ V 0.1 Hz square wave with $1 \leq |\pm V| \leq 10$ in steps of 1 V.

are shown in figure 1. Here, a $4\ \mu\text{m}$ 80° LT cell filled with ZLI-3700-000 liquid crystal material (E-Merck, Darmstadt) and placed between crossed LC81 polarizers is investigated. The cell is driven with a $0.1\ \text{Hz}$ square wave voltage and each line corresponds to one of the voltage steps between ± 1 and $\pm 10\ \text{V}$.

The magnitude of the R value is voltage dependent and peaks at voltages lying between ± 3 and $\pm 4\ \text{V}$, reaching a maximum of 1.72 shade numbers. This is rationalized by considering the electro-optic response of the cell (shown in figure 2). Here, the voltage-shade number characteristics are shown (solid line) together with the gradient function for this curve (dashed line), which is seen to peak close to $\pm 3.5\ \text{V}$. It is hence in this range that the shade number of the cell is most sensitive to voltage variations.

The magnitude of the screening voltage due to impurity ions being present within the liquid crystal material can be determined from figures 1 and 2, the results being shown in figure 3. There are two parts to this curve. The first step occurs at voltages lying below $\pm 4\ \text{V}$. Here, the external field is too small to accelerate all mobile ions present within the liquid crystal material so that they reach the cell sides within the $5\ \text{s}$ interval between polarity reversals. Raising the voltage linearly increases the acceleration of the ions and hence inflates the screening voltage.

The second part occurs above $\pm 4\ \text{V}$. Here, the applied voltage is sufficiently large to accelerate all migrating ions so that they reach the cell sides within one polarity period. Since the quantity of impurity ions present within the liquid crystal material is constant, the ensuing screen-

ing voltage is independent of the externally applied field, in this case $1.12\ \text{V}$. The ionic density present in the liquid crystal material is approximated by $n = C_{\text{LC}}\Delta V/q$, where C_{LC} is the capacitance across the bulk liquid crystal material, ΔV the screening voltage and q the ionic charge.

A negative R value (charging-up of the cell) is attributed to ions being present within the polyimide layer. Application of a d.c. voltage induces charge separation and generates a voltage across the polyimide film. Upon polarity reversal, the resulting voltage initially screens the liquid crystal layer and hence reduces the effective field. Over a period of time the screening voltage reverses polarity, causing the effective voltage across the liquid crystal layer to rise. With the cell operating in the normally transparent mode, this is manifested by an increase in shade number as a function of time. Note that this process involves the diffusion of ions through a solid material over distances of typically $0.1\ \mu\text{m}$, to be compared with that of the discharge effect which concerns the movement of ions through a liquid medium over distances of $4\ \mu\text{m}$.

The characteristics of a cell displaying this effect are shown in figure 4. Here, a $4\ \mu\text{m}$ 70° LT cell filled with Merck MLC-6296 liquid crystal mixture and employing an SE-3140 polyimide together with an SE-720 hardcoat (Nissan Chemical Industries Ltd) is used. The cell is placed between crossed LC81 polarizers and an interference filter is present. The cell is driven with a $\pm V$ $0.1\ \text{Hz}$ square wave where $1 \leq |\pm V| \leq 10$ in steps of $1\ \text{V}$.

Once again, the screening effect is seen to be most apparent in the ± 3 and $\pm 4\ \text{V}$ range where the gradient

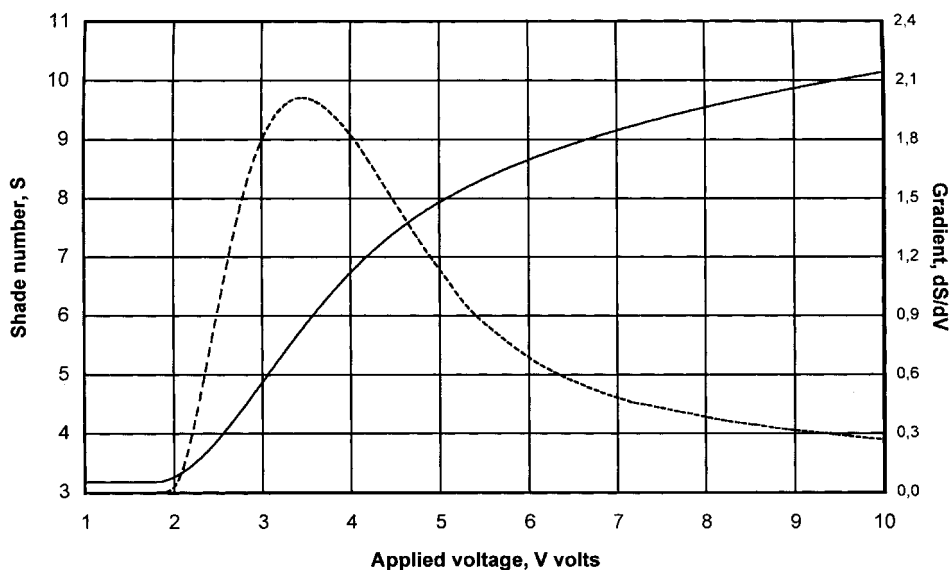


Figure 2. The electro-optic characteristics (solid line) together with the gradient function of this curve (dashed line) for the cell in figure 1 which displays a large decay effect (positive R value).

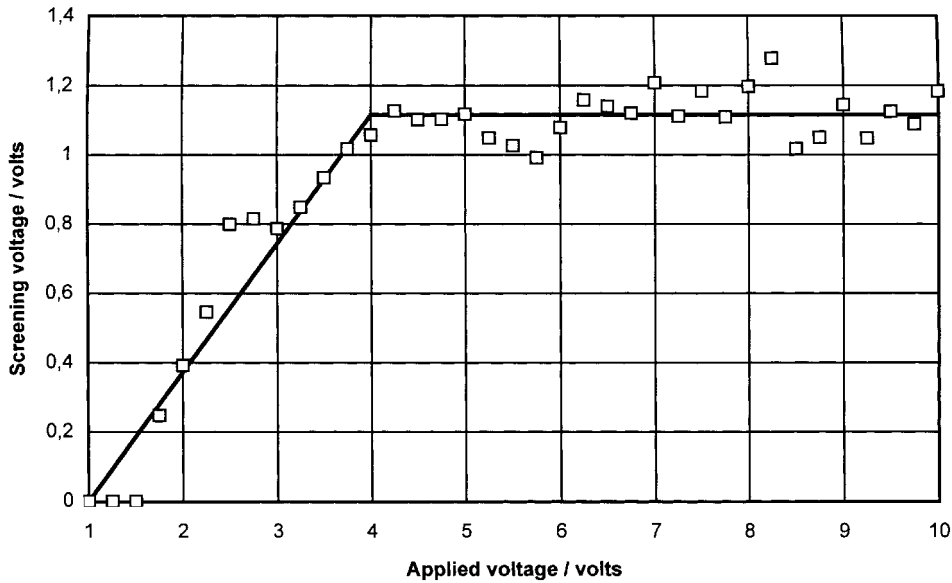


Figure 3. Screening voltage as a function of the applied driving voltage for the cell in figure 1 which displays a large decay effect due to mobile ions present within the liquid crystal material.

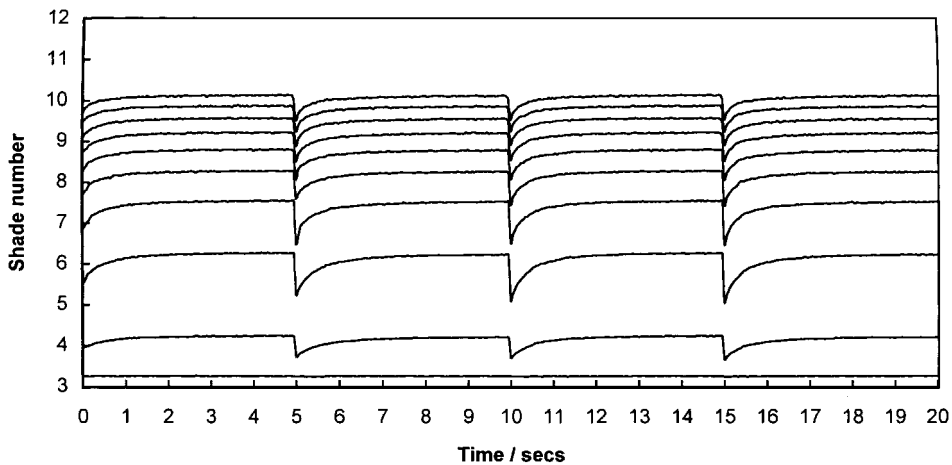


Figure 4. Charging-up effect (negative R value) in a $4\ \mu\text{m}$ 70° LT cell filled with Merck MLC-6296 liquid crystal mixture and using SE-3140 polyimide and SE-720 hardcoat. The cell is placed between crossed LC81 polarizers and an interference filter is present. The cell is driven with a $\pm V$ V 0.1 Hz square wave with $1 \leq |\pm V| \leq 10$ in steps of 1 V.

of the electro-optic curve is steepest, giving a maximum R value of -1.13 shade numbers. Figure 5 demonstrates that the screening voltage, ΔV , due to charge separation in the polyimide layer is proportional to the applied voltage, V . The field across the polyimide layer is approximated by $\Delta V = nqd/\epsilon_r\epsilon_0 A$, where d is the thickness of the film, A the surface area, ϵ_r and ϵ_0 are the relative dielectric permittivities of the polyimide material and free space, respectively, n is the total number of ions present at the surface of the layer and q the ionic charge. It is seen that $\Delta V \propto V$, inferring that $n \propto V$. Increasing the voltage raises the charge separation, but at the same time lowers the sensitivity of the shade number to

voltage variations. The net result is an R value that peaks at ± 3.5 V and becomes smaller again as the voltage is raised beyond this point. It is also noted that in order to reduce the charging-up effect to a minimum, a thinner polyimide layer with a higher electrical permittivity is required.

The magnitude of the screening voltage upon polarity reversal depends upon the polarity and extent to which charge separation has occurred within the polyimide layer immediately prior to cell switching. Figure 6 shows the optical response of the $4\ \mu\text{m}$ 70° LT cell being driven with a 0.1 Hz square wave between -10.40 and $+4.00$ V. The cell is placed between crossed LC81 polarizers and

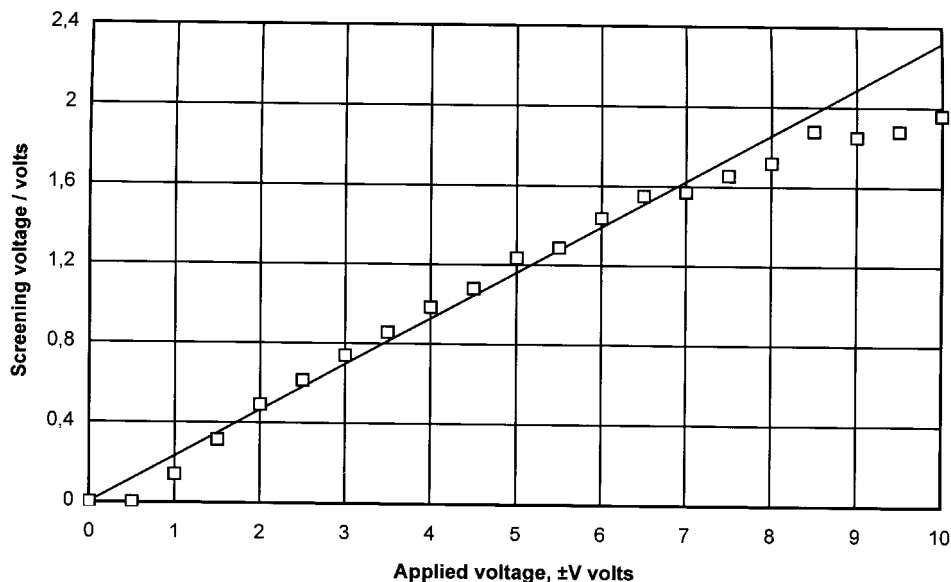


Figure 5. Shielding voltage as a function of the externally applied field arising due to charge separation occurring within the polyimide layer. A $4\mu\text{m}$ 70° LT cell with Merck MLC-6296 liquid crystal mixture, SE-3140 polyimide and SE-720 hardcoat is used. The cell is driven with a $\pm V$ 0.1 Hz square wave.

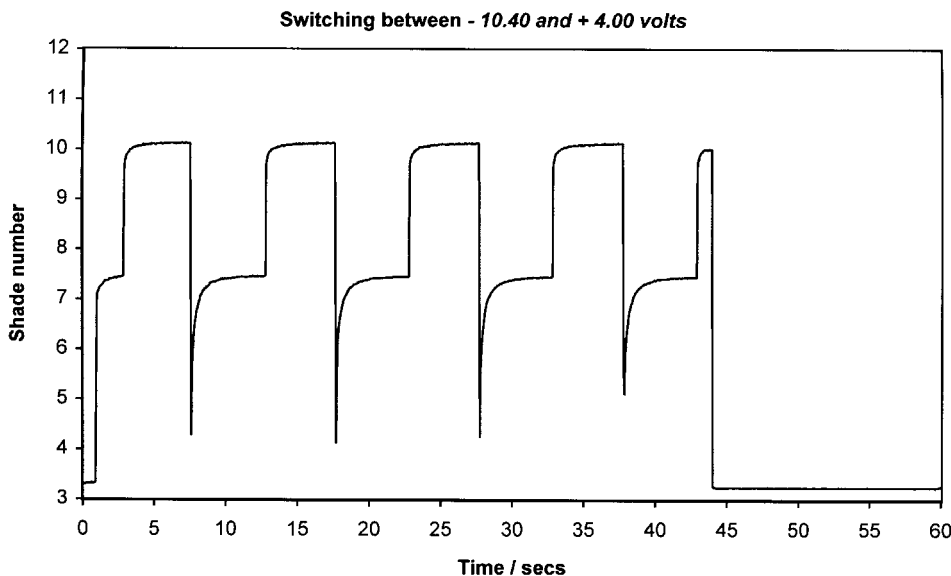


Figure 6. Large negative R value from the $4\mu\text{m}$ 70° LT cell with Merck MLC-6296 liquid crystal mixture, SE-3140 polyimide and SE-720 hardcoat. The cell is driven with a 0.1 Hz square wave between -10.40 and $+4.00$ V. The cell is placed between crossed LC81 polarizers and an interference filter is present.

an interference filter is present. Here, the externally applied -10.40 V first induces charge separation within the polyimide layer with the opposite polarity, which then initially shields the liquid crystal layer immediately after reversal of the externally applied voltage, producing a large negative R value, in this case exceeding -3.08 shade numbers.

However, the situation when the cell is switched between $+9.97$ and $+4.00$ V is shown in figure 7. Here,

the charge separation initially set up within the polyimide layer with the $+9.97$ V prior to cell switching has the opposite polarity to the $+4.00$ V to which the cell is finally switched. In this case, the voltage across the polyimide layer initially enhances the field acting over the liquid crystal material before charge separation within the polyimide layer decreases to the levels appropriate with $+4.00$ V applied to the cell, generating a positive R value of $+0.68$ shade numbers.

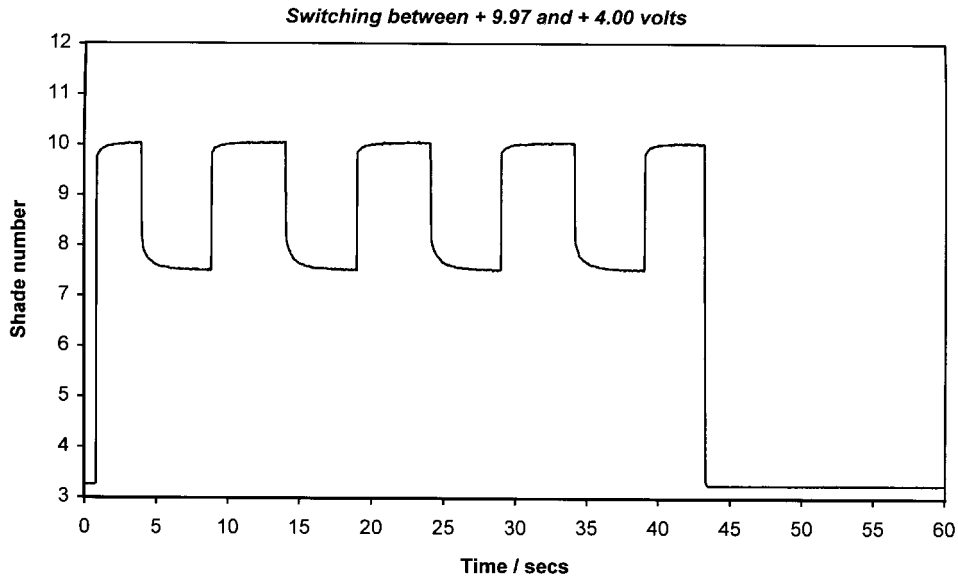


Figure 7. Positive R value from the $4\ \mu\text{m}$ 70° LT cell with Merck MLC-6296 liquid crystal mixture, SE-3140 polyimide and SE-720 hardcoat being driven with a $0.1\ \text{Hz}$ square wave between $+9.97$ and $+4.00\ \text{V}$. The cell is placed between crossed LC81 polarizers and an interference filter is present.

Figure 8 shows the magnitude of the R value as a function of the initially applied voltage for the $4\ \mu\text{m}$ 70° LT cell driven with a $0.1\ \text{Hz}$ square wave switching between V and $+4.00\ \text{V}$. With an initial voltage of $V = 4.00\ \text{V}$, the R value is zero and becomes positive for initial voltages exceeding $+4.00\ \text{V}$ and negative for starting voltages lower than this.

Cell asymmetry occurs due to there being different quantities of embedded ions present within the layers at

each side of the cell. This generates a locked-in d.c. voltage across the cell that either adds to or subtracts from the externally applied field and hence changes the effective voltage acting upon the liquid crystal layer in a way that is dependent upon the polarity. The characteristics of a cell displaying predominantly asymmetric behaviour are shown in figure 9.

Figure 10 shows the magnitude of the locked-in d.c. holding voltage as a function of the externally applied

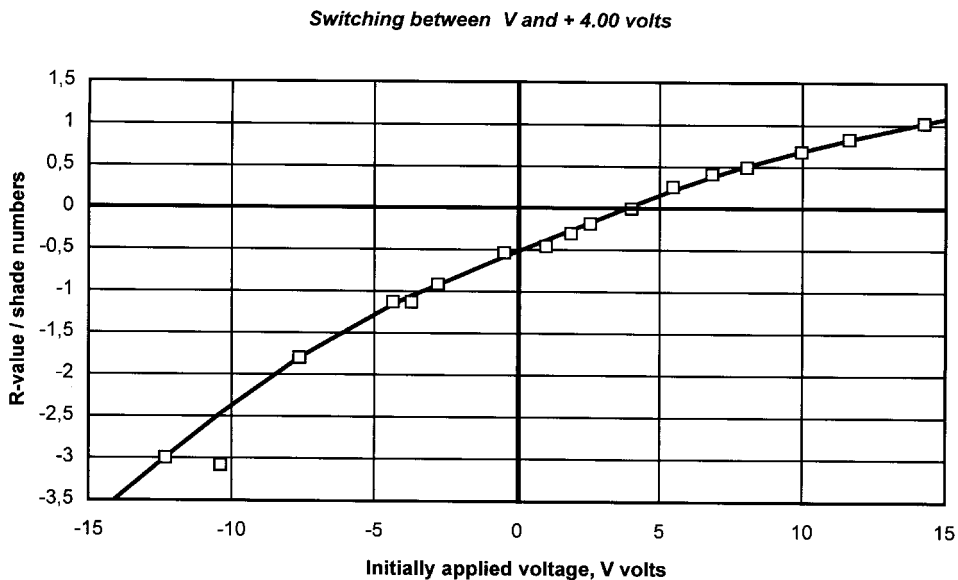


Figure 8. Magnitude of the R value due to charge separation occurring within the polyimide layer for the $4\ \mu\text{m}$ 70° LT cell driven with a $0.1\ \text{Hz}$ square wave switching between V and $+4.00\ \text{V}$ as a function of the initial externally applied field, V . The cell is placed between crossed LC81 polarizers and an interference filter is present.

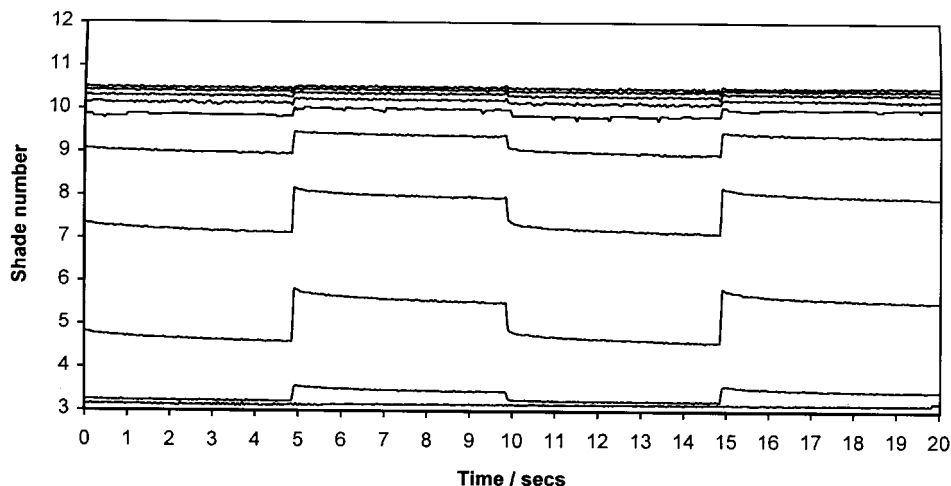


Figure 9. Cell asymmetry due to different quantities of embedded ions trapped in the alignment layers at each side of the cell.

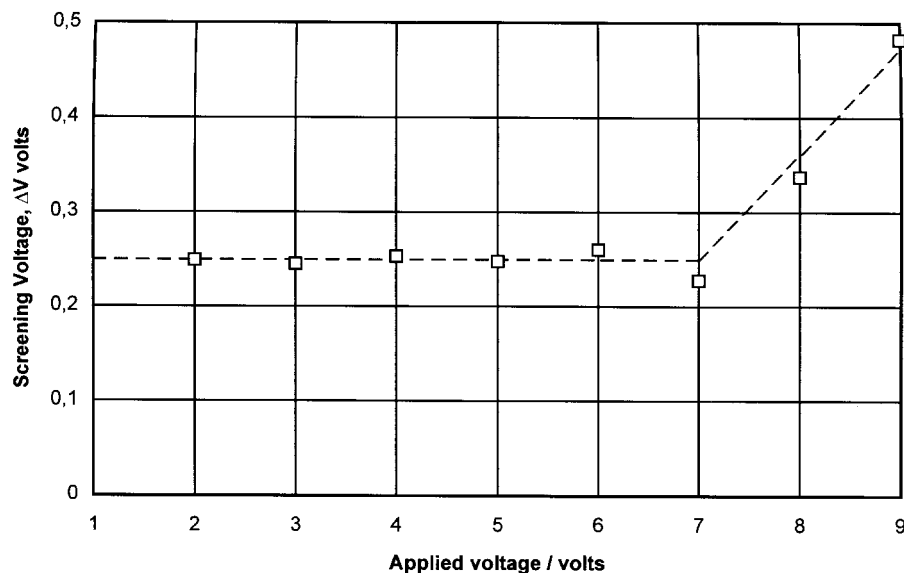


Figure 10. Locked-in d.c. holding voltage as a function of the externally applied field giving rise to cell asymmetry.

field. For voltages of less than ± 7 V, the d.c. holding voltage is independent of the applied field, in this case 0.26 V. As the voltage is increased beyond this point, the d.c. holding voltage is seen to rise. Figure 11 demonstrates that the asymmetry of the cell peaks close to ± 3.0 V, coinciding with the gradient maximum of the voltage–shade number curve.

In general, the overall low frequency response of a cell will involve a combination of all three effects whereby the net result of the oppositely competing charging-up and discharging effects are superimposed upon the asymmetry result. The response of a cell displaying both a large negative R value and a high asymmetry is shown in figure 12.

These three physical effects are summarized in a single model of the liquid crystal cell (shown in figure 13). Here, the layers of charges in both the liquid crystal

material and the polyimide film are shown. The effective voltage across the bulk liquid crystal material is given by $V_{\text{effective}} = V_{\text{ext}} - V_{1\text{poly}} - V_{2\text{poly}} - V_{\text{ions}}$. Depending upon the polarities of $V_{1\text{poly}}$, $V_{2\text{poly}}$ and V_{ions} , these voltages can either enhance or reduce the field acting on the liquid crystal molecules. The magnitudes of $V_{1\text{poly}}$, $V_{2\text{poly}}$ and V_{ions} are time dependent, giving the low frequency response of the device.

The treatment of a cell immediately prior to low frequency testing affects the response of the device. The long term driving of the cell with a 0.1 Hz square wave voltage can liberate ions from the polyimide layer into the liquid crystal material as well as enhance the dissociation reactions of both the liquid crystal molecules and of neutral impurities, resulting in a reduction of the charging-up effect and an increase of the cell discharge phenomenon. The short circuiting of the cell for several

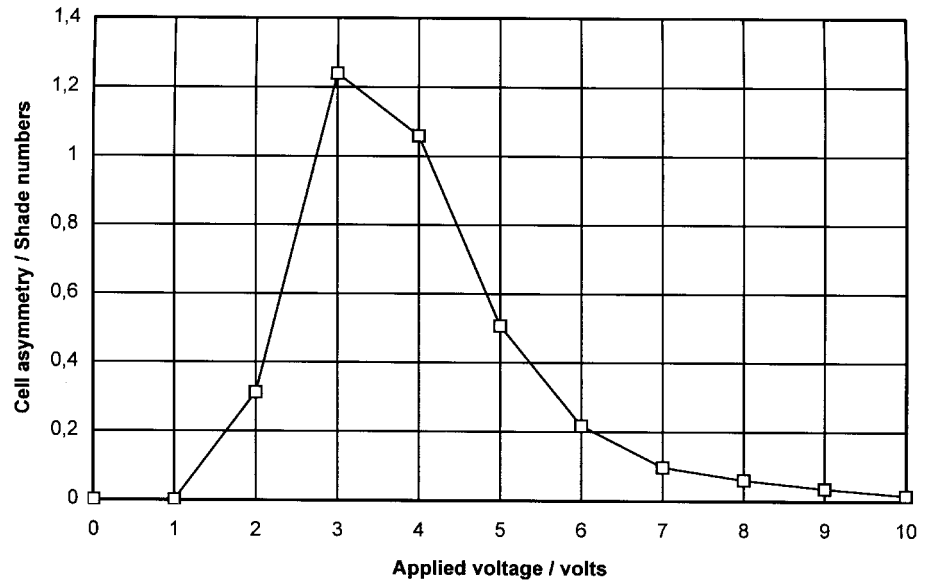


Figure 11. Magnitude of the cell asymmetry as a function of the externally applied voltage.

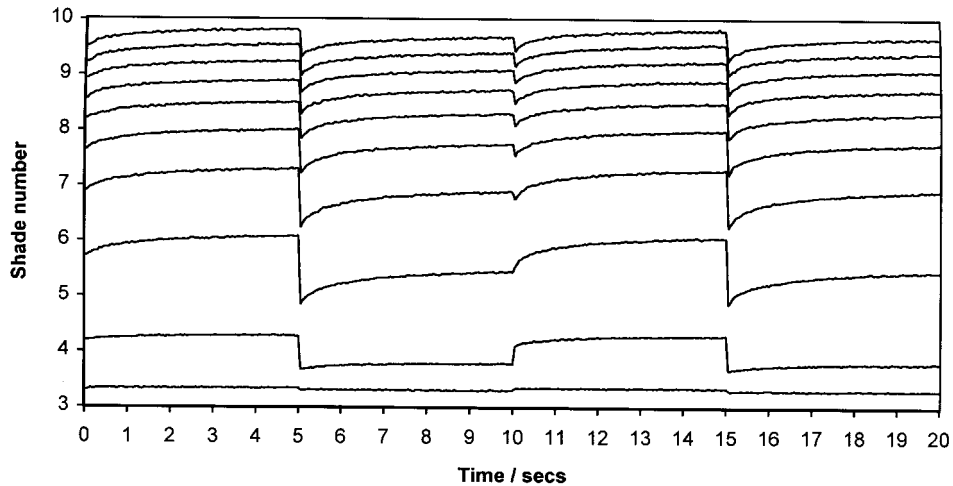


Figure 12. Optical response of a cell to a 0.1 Hz square wave voltage. The cell displays both a large negative R value and a high asymmetry.

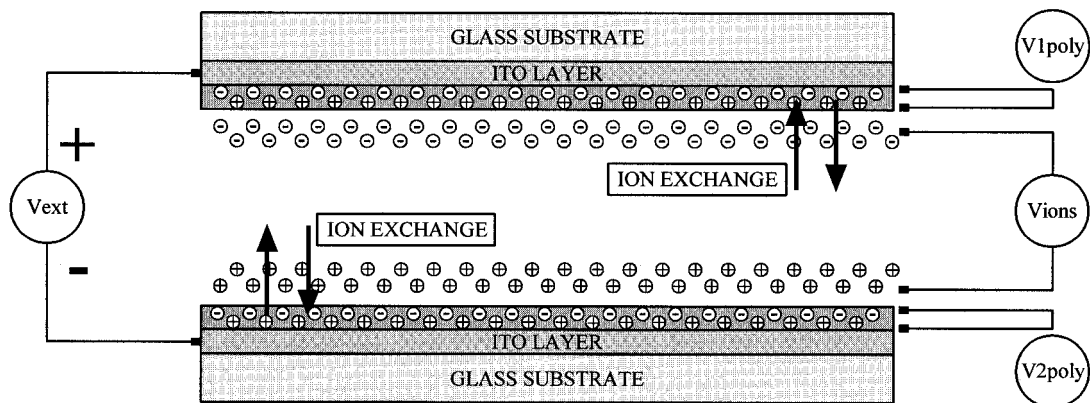


Figure 13. Model of a liquid crystal cell showing the layers of charges in both the polyimide film and the liquid crystal material. The adsorption and release of ions from the polyimide layer into the liquid crystal material is also considered in the model.

hours afterwards results in the reverse process occurring as mobile ions present within the liquid crystal material become trapped at the polyimide surface. This is demonstrated in figure 14 which shows the low frequency response of a $4\ \mu\text{m}$ 70° LT cell with the SE-3140 polyimide, the AT-2014 hardcoat and filled with MLC-6296 liquid crystal material. The thickness of the polyimide film was estimated to be 120 nm. The low frequency response of the cell directly after manufacturing is shown in figure 14(a). That when the cell has been driven with a $\pm 10\ \text{V}$ $0.1\ \text{Hz}$ square wave for a period of 1922 h at

70°C and with a relative humidity of 60% is shown in figure 14(b); figure 14(c) shows the response of the same cell having been short-circuited afterwards for a period of 8 h.

The heating of the cell at high temperatures above 150°C for several hours can increase the ionic density in the liquid crystal material, resulting in an enhancement of the cell decay effect. This occurs due to either an increase in the ions dissolved in the liquid crystal material from the polyimide layers or from an increase in the dissociation of neutral liquid crystal molecules.

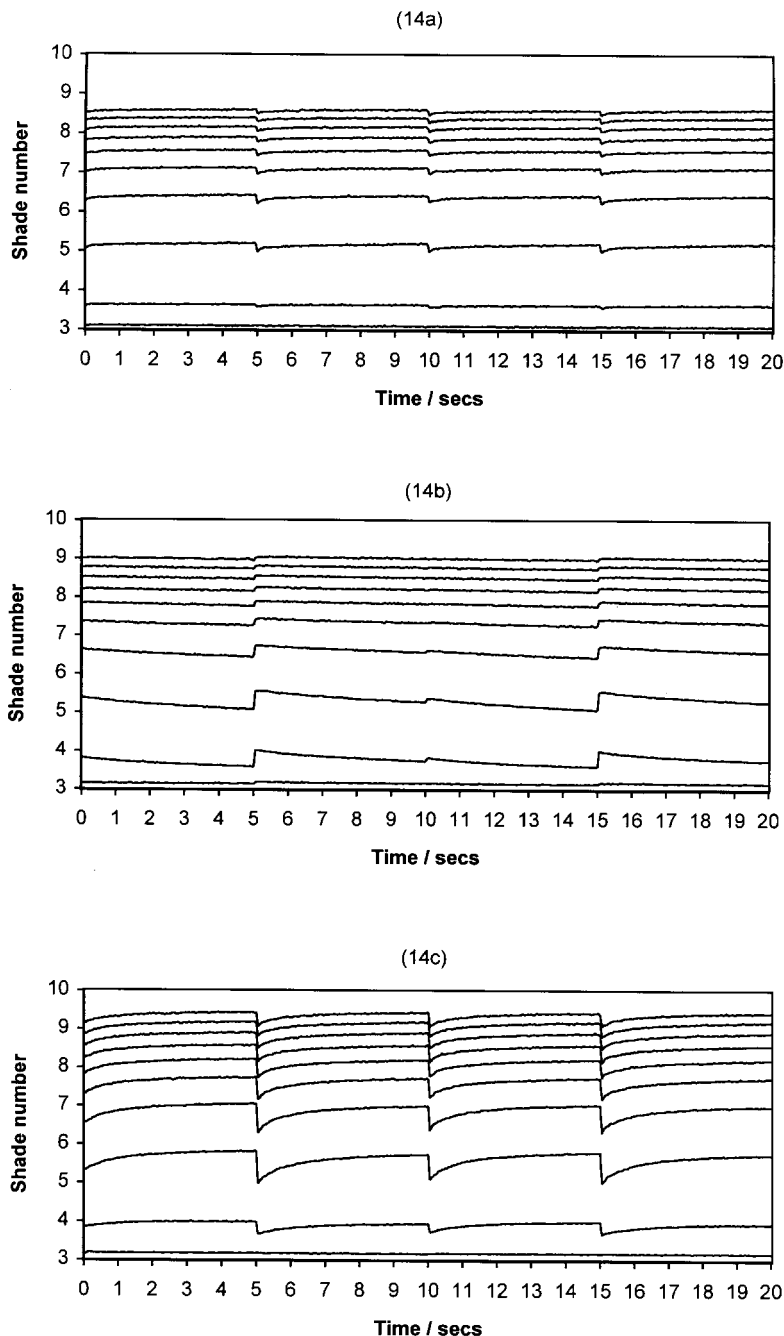


Figure 14. The low frequency response of a $4\ \mu\text{m}$ 70° LT cell with SE-3140 polyimide, AT-2014 hardcoat and filled with MLC-6296 liquid crystal material. (a) Shows the low frequency response directly after manufacturing of cell; (b) shows the response after driving the cell with a $\pm 10\ \text{V}$ $0.1\ \text{Hz}$ square wave for 1922 h at 70°C and with a relative humidity of 60%; (c) shows the response after short-circuiting of the cell afterwards for 8 h.

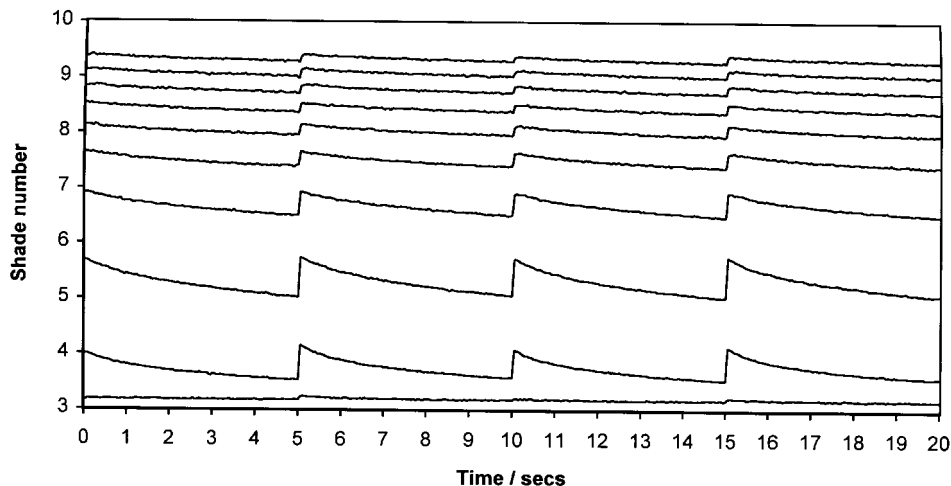


Figure 15. Low frequency response of a $4\ \mu\text{m}$ 70° LT cell with MLC-6296 liquid crystal material, SE-3140 polyimide and AT-2014 hardcoat after heating for 3 h at 150°C .

This is demonstrated in figure 15 which shows the low frequency response of the above cell after having been short circuited for 8 h followed by heating for 3 h at 150°C . It is seen that although the cell initially displays the charging-up effect due to ions being present within the polyimide layer, as demonstrated in figure 14(c), the baking of the cell generates the discharge phenomenon. Finally, it is noted that the application of a d.c. voltage to the cell for several hours drives ions into the polyimide layer, resulting in a locked-in d.c. holding voltage being present, thereby producing a high cell asymmetry.

4. Conclusions

This study demonstrates that there are predominantly three physical phenomena that occur when operating liquid crystal cells with a low frequency voltage. The first is the discharge of the device whereby the effective voltage acting on the liquid crystal material decreases as a function of time due to ions present within the liquid crystal material. The second is the charging-up of the cell, attributed to charge separation occurring within the polyimide layer. The third effect is that of cell asymmetry where the effective voltage depends upon the polarity of the externally applied field and occurs due to the presence of a locked-in d.c. holding voltage.

The low frequency response of the cell can be deduced by considering the movement of ions within the device. The long term operation of the cell liberates ions from the polyimide layers into the liquid crystal material and the discharge effect becomes dominant. Short-circuiting of the cell afterwards generates the reverse effect and the charging-up effect begins to take over. This is a semi-reversible process.

Heating of the cell at 150°C for several hours increases the ionic concentration of the liquid crystal material

and enhances the discharge phenomenon. Finally, the addition of a d.c. voltage for prolonged periods of time drives ions into the polyimide layer. These ions become embedded, generating a locked-in d.c. holding voltage and giving rise to a large cell asymmetry. In order to manufacture cells suitable for low frequency driving, the ionic content of the liquid crystal material must be kept to a minimum and thin polyimide layers must be used. Operation of a liquid crystal cell above the voltage region for which the gradient of the electro-optic curve is greatest also reduces the perceived R value and asymmetry.

References

- [1] SEIBERLE, H., and SCHADT, M., 1992, *SID92*, International Symposium Digest of Technical Papers, **XXIII**, 25.
- [2] SCHADT, M., 1994, *SID94*, International Display Research Conference, pp. 96–102.
- [3] COLPAERT, C., MAXIMUS, B., and PAUWELS, H., 1993, *Euro Display 93* (Proc. 13th Int. Disp. Res. Conf.), pp. 301–304.
- [4] MUGRIDGE, R. J., GIBBONS, D. J., 1992, *Japan Display 92* (Proc. 12th Int. Disp. Res. Conf.), pp. 583–586.
- [5] COLPAERT, C., DE MEYERE, A., VERWEIRE, B., ZHANG, H., and PAUWELS, H., 1997, *SID97*, International Symposium Digest of Technical Papers, **XXVIII**, 195.
- [6] COLPAERT, C., MAXIMUS, B., and GROENEVELD, C. M., 1994, *SID94*, International Display Research Conference, pp. 191–194.
- [7] MAXIMUS, B., and COLPAERT, C., 1995, *SID95*, International Symposium Digest of Technical Papers, **XXVI**, 609.
- [8] MAXIMUS, B., VETTER, P., and PAUWELS, H., 1991, Proc. 11th Int. Disp. Res. Conf. (San Diego '91), pp. 53–56.
- [9] NAEMURA, S., NAKAZONO, Y., ICHINOSE, H., and SAWADA, A., 1997, *SID97*, International Symposium Digest of Technical Papers, **XXVIII**, 199.

- [10] FEHLNER, F. P., SALISBURY, K. R., and BINKOWSKI, N. J., 1995, *SID95*, International Symposium Digest of Technical Papers, **XXXVI**, 771.
- [11] COLPAERT, C., MAXIMUS, B., and DE MEYERE, A., 1996, *SID96*, International Symposium Digest of Technical Papers, **XXVII**, 301.
- [12] COMPAERT, C., DE MEYERE, A., and VERWEIRE, B., 1996, *Euro Display 96* (Proc. 16th Int. Disp. Res. Conf.), pp. 325–329.
- [13] HASEGAWA, M., TAKANO, H., TAKENAKA, A., MOMOI, Y., NAKAYAMA, K., and LIEN, A., 1995, *SID96*, International Symposium Digest of Technical Papers, **XXVII**, 666.
- [14] KITAMURA, M., 1996, *Euro Display 96* (Proc. 16th Int. Disp. Res. Conf.), pp. 330–333.
- [15] TAKAHASHI, S., MIYAKE, S., TOBITA, T., and TAKASAGO, H., 1992, *Japan Display 92* (Proc. 12th Int. Disp. Res. Conf.), pp. 639–642.
- [16] GROENEVELD, C. M., 1993, *Euro Display 93* (Proc. 13th Int. Disp. Res. Conf.), pp. 211–214.
- [17] LIEN, A., CHEN, C. J., INOUE, H., and SAITOH, Y., 1997, *SID97*, International Symposium Digest of Technical Papers, **XXVIII**, 203.
- [18] *European Standard EN 169*, 1992, 'Personal eye protection—Filters for welding and related techniques—Transmittance Requirements and Recommended Utilisation'.